www.czasopisma.pan.pl PAN POLSKA AKADEMIA NAUK www.journals.pan.pl

Arch. Metall. Mater. **64** (2019), 4, 1249-1255

DOI: 10.24425/amm.2019.130087

J. MIETTINEN*, V-V. VISURI*, T. FABRITIUS*, N. MILCHEVA**, G. VASSILEV***#

THERMODYNAMIC DESCRIPTION OF TERNARY Fe-B-X SYSTEMS. PART 6: Fe-B-Ti

Thermodynamic optimizations of the ternary Fe-B-Ti system and its binary sub-system, B-Ti are presented. The thermodynamic descriptions of the other binaries, Fe-Ti and Fe-B, are taken from the earlier studies slightly modifying the Fe-Ti system assessment. The adjustable parameters of the Fe-B-Ti and B-Ti systems are optimized in this study using the experimental thermodynamic and the phase equilibrium data from the literature. The solution phases of the system are described using the substitutional solution model and the compounds (including borides) are treated as stoichiometric phases. The results show a good correlation between the calculated and measured thermodynamic and phase equilibrium data.

Keywords: phase diagrams; thermodynamic modeling; Fe based systems; Fe-B-X systems thermodynamic database; Fe-B-Ti system

1. Introduction

The current work continues the earlier started project [1] related to the development of boron containing iron-based Fe-B-X database, where boron is treated as a substitutional component. The previous contributions Fe-B-Cr [1], Fe-B-Ni [2], Fe-B-Mn [3], Fe-B-V [4], published earlier are followed by the current ternary Fe-B-Ti description. The purpose is to develop a simple and compatible thermodynamic database for steels, which provides important and practical input data for thermodynamic-kinetic models simulating their solidification. Thus, any complex phase descriptions published in the literature are beyond the scope of this database. The new Fe-B-Ti description can be applied in modeling of solidification and grain structure formation in various steels [5,6].

In this sixth part, a thermodynamic description is of the ternary Fe-B-Ti system and its binary sub-system B-Ti is conducted using experimental (or assessed) thermodynamic and phase equilibrium data from the literature. The other binary thermodynamic parameters used in the current Fe-B-Ti description are taken from [1] for Fe-B and from [7,8] for Fe-Ti. The descriptions of the liquid Fe-Ti phase and Fe_2Ti [8], however, were slightly modified in this study to achieve a better agreement with the measured mixing enthalpies in liquid and to facilitate the treatment of the Fe_2Ti phase in other systems. Additionally, a simple temperature function was used for the FeTi molar Gibbs energy of formation.

Although a description of the Fe-Ti system has been recently published by Bo et al. [9], that study applies more refined sublattice treatments (for the Fe_2Ti and FeTi phases), which are beyond the scope of our database.

The Fe-B-Ti system was earlier assessed by Tanaka and Saito [10] but quite tentatively and using binary data different from those of the current database. The B-Ti system has also been assessed earlier [11-13]. Nevertheless, these descriptions assume a stable TiB_2 phase, which results in a poor description of the L + TiB_2 equilibrium in iron-rich Fe-B-Ti alloys. Consequently, the whole system should be reassessed using a simple temperature expression for the stoichiometric boride, TiB_2.

2. Phases, modeling and data

Table 1 shows the phases and their modeling in the current Fe-B-Ti assessment. The solution phases (*L*, *bcc*, *fcc*, *hcp*) are described with the substitutional solution model and the binary compounds, including borides, are treated as stoichiometric phases. No solubility of Fe or Ti in the rhombohedral boron phase (referred to as “bet” bellow) is considered.

Detailed descriptions of the substitutional solution and sublattice models and their parameters are available from Qiu [14,15].

Experimental data about the pertinent systems are scarce but available and have been used for the current descriptions. For example, the experimental studies on the Fe-B-Ti system have been reviewed by Raghavan [16,17].

Rudy [18] reported differential thermal analyses data about the B-Ti system while Murray et al. [19] – assessed phase equi-

* UNIVERSITY OF OULU, PROCESS METALLURGY RESEARCH UNIT, OULU, FINLAND
** MEDICAL UNIVERSITY OF PLOVDIV, FACULTY OF PHARMACY, PLOVDIV, BULGARIA
*** UNIVERSITY OF PLOVDIV, FACULTY OF CHEMISTRY, 24 TSAR ASEN STR.,4000 PLOVDIV, PLOVDIV, BULGARIA
# Corresponding author: gpvassilev@gmail.com

TABLE 1

Phases and their modeling in the current Fe-B-Ti description

Phase	Modeling
liquid (L)	(B,Fe,Ti), substitutional, RKM[a]
bcc_A2 (bcc, base centered cubic)	(B,Fe,Ti), substitutional, RKM
fcc_A1 (fcc, face centered cubic)	(B,Fe,Ti), substitutional, RKM
hcp_A3 (hcp, hexagonal close packing)	(B,Fe,Ti), substitutional, RKM
Fe_2Ti (l)	$(Fe)_2(Ti)$, stoichiometric
FeTi	(Fe)(Ti), stoichiometric
Fe_2B	$(Fe)_2(B)$, stoichiometric
FeB	(Fe)(B), stoichiometric
TiB	(Ti)(B), stoichiometric
Ti_3B_4	$(Ti)_3(B)_4$, stoichiometric
TiB_2	$(Ti)(B)_2$, stoichiometric
beta-rhombo-B (bet)	(B)

[a] – RKM – Redlich-Kister-Muggianu (Gibbs excess energy model).

libria data. Enthalpy of formation of solid B-Ti alloys, at 25°C has been assessed by various authors [20-25] while estimated Gibbs energies of formation of TiB_2 have been presented also [26,27]. Entropy of formation of solid alloys, at 25°C [22,28] and heat capacity of TiB_2 have been reported as well [29].

Concerning the ternary system, four isothermal sections, at 1450, 1290, 1175 and 1050°C from Ottavi et al. [30] and from A. Antoni-Zdziobek et al. [31] have been used in the optimization, as well as one vertical section, at molar ratio $x_B:x_{Ti} = 2$ from Ottavi et al. [30] and Shurin and Panarin [32].

Moreover, experimental data of the Fe-Ti phase equilibria [7,14,15,33-46], the mixing enthalpy of liquid Fe-Ti alloys [47-49], the chemical potentials of Fe and Ti in the liquid alloys [50,51], and the enthalpy of formation of Fe_2Ti and FeTi [52,53] were used for the partial re-optimization of the Fe-Ti system.

3. Results

The thermodynamic description of the Fe-B-Ti system is shown in Table 2. The parameters marked with a reference code were taken from the earlier assessments and the rest were optimized (O*) using experimental data or estimated (E*) since no experimental data are available.

The calculated results are compared with the original experimental data to verify the optimization. All calculations were carried out using the ThermoCalc software [57].

Figsures 1 to 3 show the calculated Fe-B phase diagram [1] and the Fe-Ti and B-Ti phase diagrams reassessed in the current study, respectively. The agreement with the experimental data is reasonable. In Table 3 more details about the calculated and the experimental invariant points of the B-Ti system have been compiled.

TABLE 2

Thermodynamic description of the Fe-B-Ti system. Thermodynamic data of pure components are taken from the literature [54] unless shown otherwise in the table. Parameter values except for *Tc* and β are in J/mol. *Tc* and β are the Curie temperature (K) and the effective magnetic moment (magneton), of a phase, respectively

liquid (1 sublattice, sites: 1, constituents: B,Fe,Ti)	Ref.
$L^L_{B,Fe} = (-133438 + 33.946T) + (+7771)(x_B - x_{Fe}) + (+29739)(x_B - x_{Fe})^2$	[55]
$L^L_{B,Ti} = (-265000 + 15.5T) + (-134000 + 17.7T)(x_B - x_{Ti}) + + (+73000)(x_B - x_{Ti})^2 + (+60000)(x_B - x_{Ti})^3$	O*
$L^L_{Fe,Ti} = (-78500 + 13.2T) + (+300)(x_{Fe} - x_{Ti}) + (+13300)(x_{Fe} - x_{Ti})^2$	O*
$L^L_{B,Fe,Ti} = (-100000 + 60T)x_B + (-275000 + 60T)x_{Fe} + (-100000 + 60T)x_{Ti}$	O*
bcc (1 sublattice, sites: 1, constituents: B,Fe,Ti)	
${}^oG^{bcc}_B = {}^oG^{bet}_B + (+43514 - 12.217T)$	[56]
$L^{bcc}_{B,Fe} = (-50000 + 42T)$	[1]
$L^{bcc}_{B,Ti} = (-87000)$	O*
$L^{bcc}_{Fe,Ti} = (-59098 + 11.5T) + (-1796 + 1T)(x_{Fe} - x_{Ti}) + (+5602 + 3.5T)(x_{Fe} - x_{Ti})^2$	[7]
$Tc^{bcc} = 1043x_{Fe}$	[54]
$\beta^{bcc} = 2.22x_{Fe}$	[54]
fcc (1 sublattice, sites: 1, constituents: B,Fe,Ti)	
${}^oG^{fcc}_B = {}^oG^{bet}_B + (+50208 - 13.478T)$	[56]
$L^{fcc}_{B,Fe} = (-66000 + 50T)$	[1]
$L^{fcc}_{B,Ti} = L^{bcc}_{B,Ti}$ (*fcc* not stable in binary B – Ti)f	E*
$L^{fcc}_{Fe,Ti} = (-51625 + 11T) + (-1950 - 6T)(x_{Fe} - x_{Ti}) + (+14875)(x_{Fe} - x_{Ti})^2$	[7]
$Tc^{fcc} = -201x_{Fe}$	[54]
$\beta^{fcc} = -2.1x_{Fe}$	[54]
hcp (1 sublattices, sites: 1, constituents: B,Fe,Ti)	
${}^oG^{hcp}_B = {}^oG^{bet}_B + (+50208 - 13.478T)$	[56]
$L^{hcp}_{B,Ti} = L^{bcc}_{B,Ti}$	O*
$L^{hcp}_{Fe,Ti} = (-28750 + 11T) + (-1700 - 6T)(x_{Fe} - x_{Ti}) + (+15000)(x_{Fe} - x_{Ti})^2$	[10]
Fe_2Ti (l) (2 sublattices, sites: 2:1, constituents: Fe:Ti)	
$G^l_{Fe:Ti} = 2{}^oG^{bcc}_{Fe} + {}^oG^{hcp}_{Ti} + (-83918 - 4.764T + 2.3644T\ln T + 0.00016T^2)$	O*

FeTi (2 sublattices, sites: 1:1, constituents: Fe:Ti) ${}^{o}G^{FeTi}_{Fe:Ti} = {}^{o}G^{bcc}_{Fe} + {}^{o}G^{hcp}_{Ti} + (-53693 - 8.819T + 1.6717T\ln T + 0.00106T^{-2})$	[8]#
Fe_2B (2 sublattices, sites: 2:1, constituents: Fe:B) ${}^{o}G^{Fe2B}_{Fe:B} = 2{}^{o}G^{bcc}_{Fe} + {}^{o}G^{bet}_{B} + (-78783 + 10.398T)$ ${}^{o}G^{Fe2B}_{Ti:B} = 2{}^{o}G^{hcp}_{Ti} + {}^{o}G^{bet}_{B} + (-90000 + 45T)$ $L^{Fe2B}_{Fe,Ti:B} = (-240000)$	[55] O* O*
FeB (2 sublattices, sites: 1:1, constituents: Fe:B) ${}^{o}G^{FeB}_{Fe:B} = {}^{o}G^{bcc}_{Fe} + {}^{o}G^{bet}_{B} + (-70300 + 12T)$	[1]
TiB (2 sublattices, sites: 1:1, constituents: Ti:B) ${}^{o}G^{TiB}_{Ti:B} = {}^{o}G^{hcp}_{Ti} + {}^{o}G^{bet}_{B} + (-163000 + 4T)$	O*
Ti_3B_4 (2 sublattices, sites: 3:4, constituents: Ti:B) ${}^{o}G^{Ti3B4}_{Ti:B} = 3{}^{o}G^{hcp}_{Ti} + 4{}^{o}G^{bet}_{B} + (-644000 + 25T)$	O*
TiB_2 (2 sublattices, sites: 1:2, constituents: Ti:B) ${}^{o}G^{TiB2}_{Ti:B} = {}^{o}G^{hcp}_{Ti} + 2{}^{o}G^{bet}_{B} + (-287000 + 5T)$	O*

O[a] – Parameter optimized in this work
E[b] – parameter estimated in this work
– Simplified function. The reference states of Fe and Ti changed from HSER of [8].

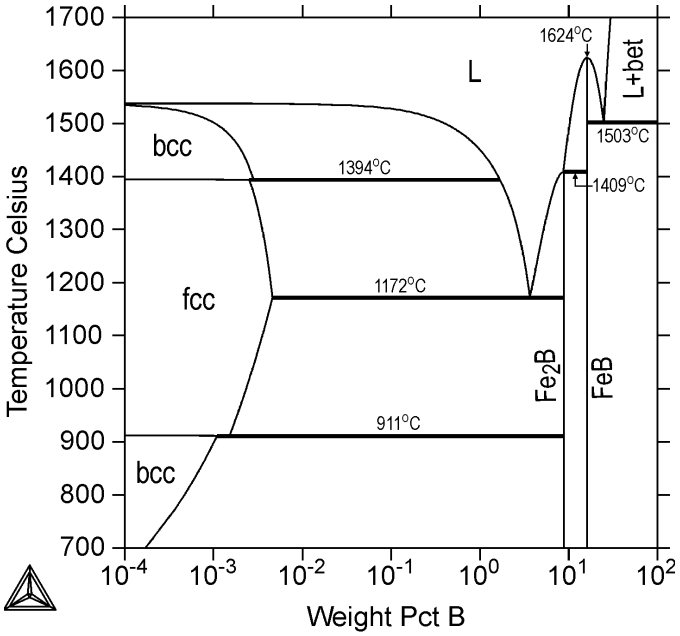

Fig. 1. Calculated [1] Fe-B phase diagram

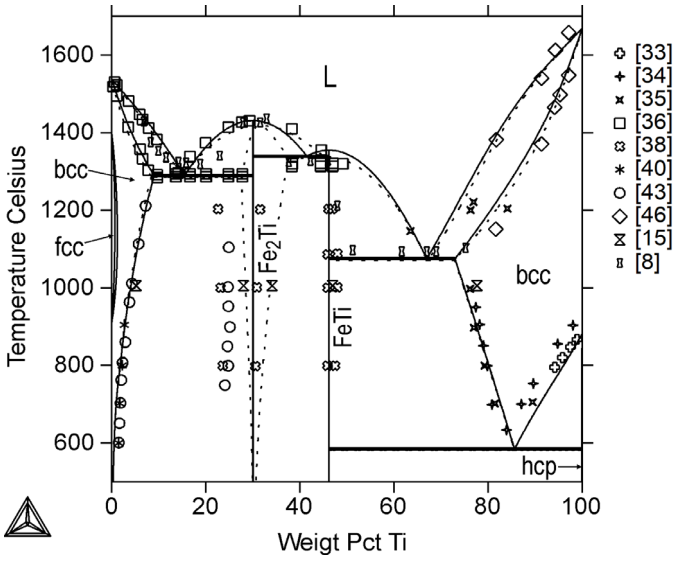

Fig. 2. Calculated Fe-Ti phase diagram, together with experimental data points [7,15,33-36, 38,40,43,46]. Solid lines refer to the current assessment and dotted lines refer to that of Lee [8]

TABLE 3

Calculated (calc) and experimental (exp) invariant points of the B-Ti system. $C_B^{\phi i}$ denotes the B concentration in an equilibrium phase ϕi

$\phi 1 - \phi 2 - \phi 3$	t °C	$C_B^{\phi 1}$ wt%	$C_B^{\phi 2}$ wt%	$C_B^{\phi 3}$ wt%	Reference
L = *bcc* + TiB	1534 1540	1.928 1.671	0.060 —	18.419 17.246	calc This study exp [19]
L + Ti_3B_4 = TiB	2156 2160	13.705 13.082	23.138 23.138	18.419 17.826	calc This study exp [19]
L + TiB_2 + Ti_3B_4	2199 2190	14.260 14.052	31.111 28.641	23.138 23.138	calc This study exp [19]
L = TiB_2	3233 3225	31.111 30.472	31.111 30.472		calc This study exp [19]
L = *bet* + TiB_2	2057 2080	89.275 91.710	100 100	31.111 31.431	calc This study exp [19]
bcc = TiB + *hcp*	882 884	0.0006 —	18.419 17.246	0.0002 —	calc This study exp [19]

Concerning the Fe-Ti system, which is partially re-optimized in this study, it is important to discuss the main differences between the current calculations and those of Lee [8]. It can be seen in Figure 1 that the current stoichiometric treatment of Fe_2Ti does not fit well with the experimental Fe_2Ti + FeTi + L equilibrium but gives slightly better agreement for the Fe_2Ti experimental melting point. An improved agreement with the experimental mixing enthalpy data of liquid [47-49] has been achieved using new liquid phase description (Fig. 4). In the reassessed Fe-Ti system, good agreement was obtained also between the calculated and experimental *bcc* + *fcc* region [36,37,39,41], the phase boundaries between bcc, FeTi and hcp-phases [42,44,45] (not visible in Figure 1), the chemical potentials of Fe and Ti in the liquid phase [50,51], and the enthalpies of formation of Fe_2Ti and FeTi [52,53]. The results of the current Fe-Ti system reassessment for the solid state phase equilibria are identical to those of Lee [8].

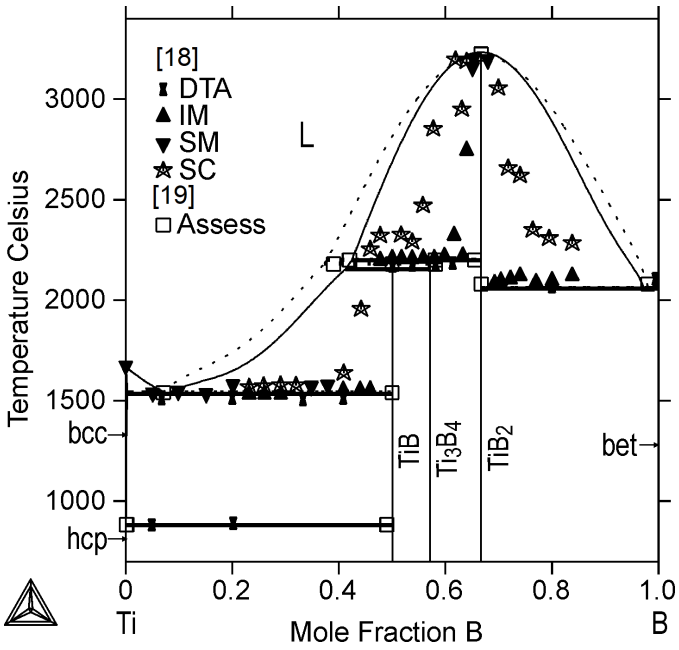

Fig. 3. Calculated B-Ti phase diagram, together with experimental data points of Rudy [18] and those assessed by Murray et al. [19]. DTA – differential thermal analysis, IM – incipient melting, SM – sharp melting, and SC – specimen collapsed. Solid lines refer to the current calculations and dotted lines refer to those of Bätzner [11]

In addition to the phase diagram of Figure 3, more results for the B-Ti system optimization are shown in Figures 5 and 6. The enthalpy of formation of solid B-Ti alloys (Figure 5) resulted from the calculations is slightly different than by that of Bätzner [11]. Particularly, note the less negative enthalpy value of the current TiB_2 description, which prevents that phase from coming too stable in the $L + TiB_2$ equilibrium appearing in the iron-rich corner of the Fe-B-Ti system. For the Gibbs energy of formation of TiB_2 (Figure 6), the calculations are in reasonable agreement with the somewhat different experimental data of [26] and [27].

For the entropy of formation of solid TiB and TiB_2 at 25°C, [22] and [28] give experimental values of 17.6 and 9.5 J/(mol·K), respectively, whereas the ones calculated by this study and Bätzner [11] are about 16.5 and 11.5 J/(mol·K). Finally, the current calculations agree reasonably well and slightly better than those of Bätzner [11] with the experimental heat capacity

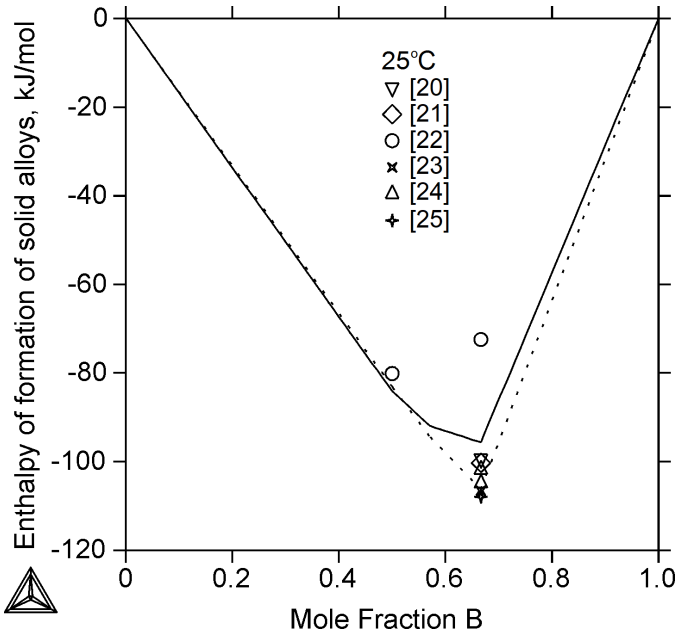

Fig. 5. Calculated enthalpy of formation of solid B-Ti alloys at 25°C, together with experimental data points [20-25]. Solid line refers to the current calculations and dotted line refers to those of Bätzner [11]. The reference states used are pure *hcp* Ti and pure beta-rhombo B

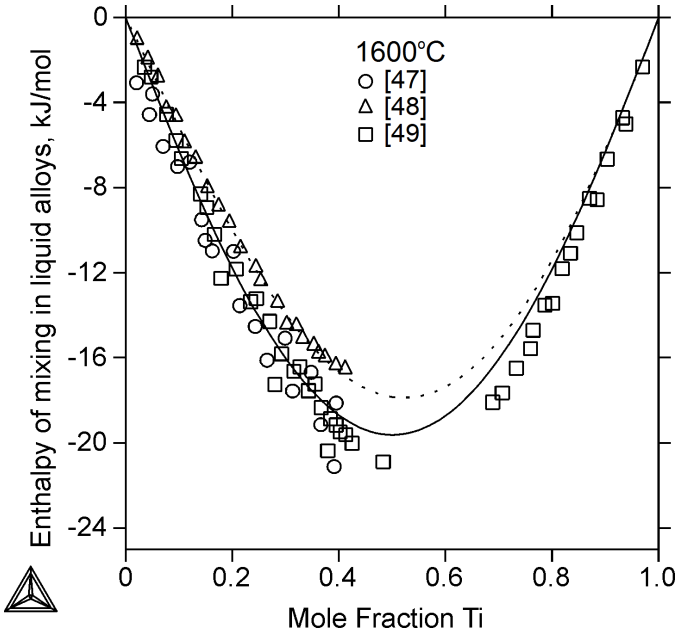

Fig. 4. Calculated enthalpy of mixing of liquid Fe-Ti alloys at 1600°C, together with experimental data points [47-49]. Solid lines refer to the current calculations and dotted lines refer to those of Lee [8]. The reference states used are pure liquid Fe and Ti

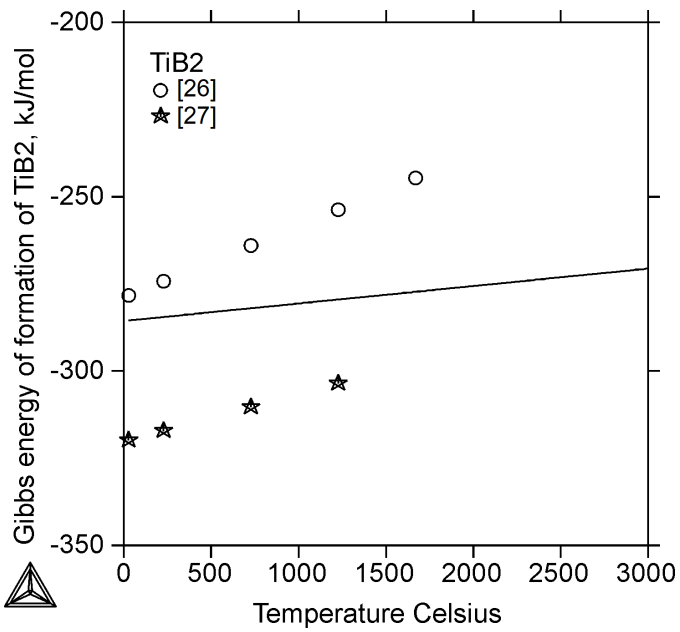

Fig. 6. Calculated Gibbs energy of formation of TiB_2, together with experimental data points [26,27]. Solid line refers to the calculations (this work) and dotted line refers to those of Bätzner [11]. The reference states used are pure *hcp* Ti and pure beta-rhombo B

of TiB_2 [29], although not that well with heat capacity data from Chase [28].

The results for the Fe-B-Ti system are shown in Table 4 and Figures 7-13. The agreement with the available experimental data is reasonably good. However, the calculated liquidus projection (Figure 7), as well as the calculated invariant points of the system (Table 4) should be considered as tentative only, which is due to the lack of systematic ternary experimental data. For the eutectic reaction of $L = fcc + Fe_2B + TiB_2$, however, two assessed points of 3.7wt%B-1170°C [30] and 0.66 wt% Ti-3.41 wt% B-1155°C [31] are available. These are not far from the calculated points of 0.94 wt% Ti, 3.90 wt% B and 1166°C.

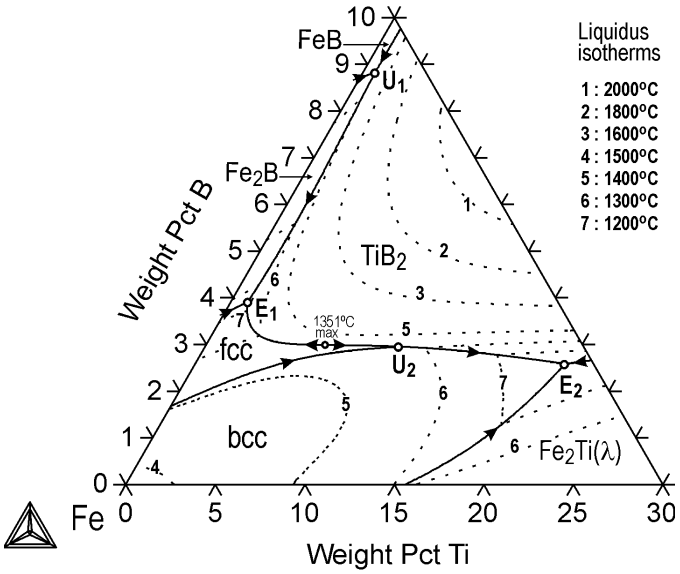

Fig. 7. Calculated liquidus projection in the Fe-rich corner of the Fe-B-Ti system. Shown also are the calculated liquidus isotherms between 2000 and 1200°C, by dotted lines

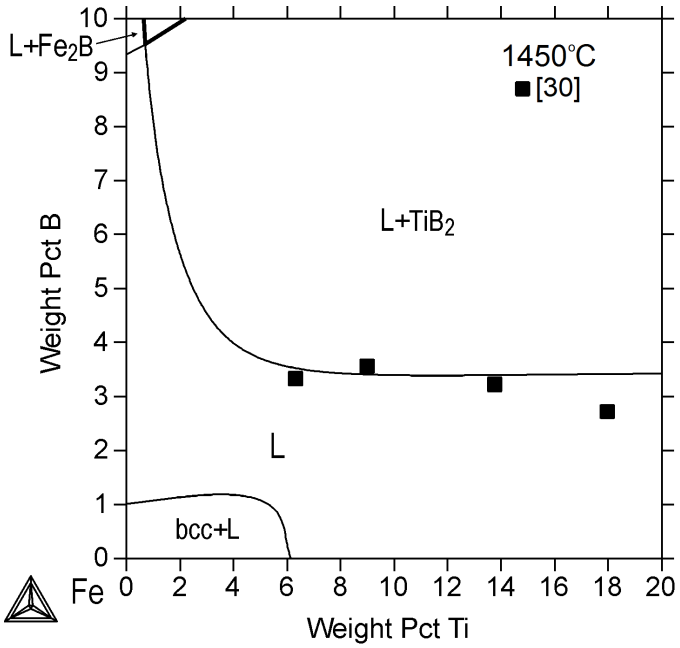

Fig. 8. Calculated isotherm of 1450°C in the Fe-B-Ti system, together with experimental data points [30]

In Figure 8, a round *bcc* + *L* region appears, due to the "strong" value of the liquid state ternary interaction parameter $L^{L}_{B,Fe,Ti}$. Using this parameter it was possible to attain a curvature for the $L/L + TiB_2$ boundary, which agrees well with the experimental data points of [30] (see Figure 8). One has to be aware that when using the Gibbs energy expressions for TiB_2 [11,12], such a curvature would be possible only by introducing a rather strong liquid ternary interaction parameter, which would cause unusual extensions for the *bcc* + *L* region in the iron rich corner. Clearly, the substitutional solution model may not be the best choice to describe the thermodynamic properties of iron-rich Fe-B-Ti alloys, but that model still seems to work well using the currently available data.

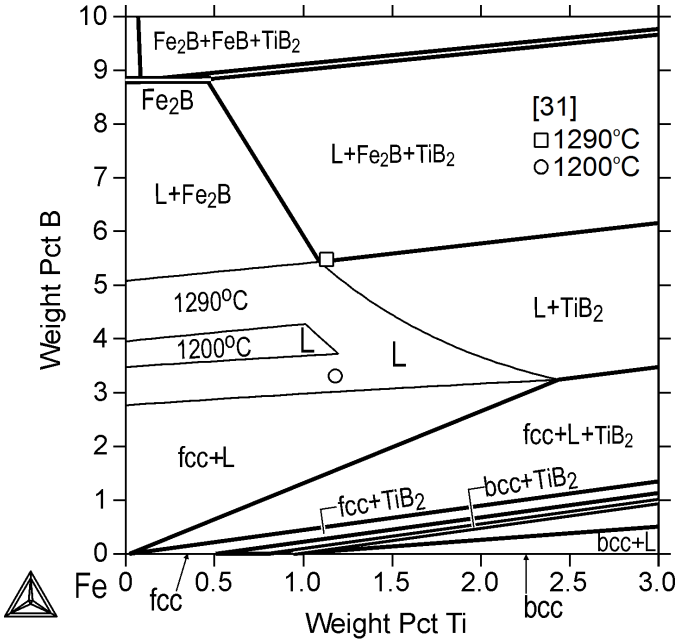

Fig. 9. Calculated isotherm of 1290°C in the Fe-B-Ti system, together with an experimental data point for the liquid phase [31]. Shown also is the liquid phase at 1200°C, with and additional experimental data point from [31]

In Figure 10, note the experimental Fe-B side three phase triangle of *fcc*-Fe_2B-*L*, not appearing by the calculations. This is due to the low Fe-B eutectic temperature by the calculations, 1172°C, supported also by [58], in regard to 1195°C suggested by [31]. That three-phase triangle, however, becomes present also by the calculations, if we lower the temperature of Figure 10 with 4°C only. An inconsistency between the experimental data from [30] and [31] resulting in different eutectic temperatures and compositions (given by the bending points of the dotted lines of the figure) is seen in Figure 12. The best compromise found in the process of optimization was to use preferably the $L/L + TiB_2$ data from [30] and the eutectic temperature by Shurin and Panarin [32].

Finally, Figure 13 shows the calculated B solubility in the *fcc* and *bcc* phases. The Ti content increase promotes the formation of TiB_2, which considerably decreases B content in these solid solutions. The boron amount is decreased also with the temperature drop from 1150 to 1000°C.

TABLE 4

Calculated invariant points in the Fe-rich corner of the Fe-B-Ti system

Reaction	Code	*t*, °C	wt% Ti in *L*	wt% B in *L*
L + FeB = Fe_2B + TiB_2	U_1	1404	0.68	8.81
L + *fcc* = *bcc* + TiB_2	U_2	1322	10.86	2.95
L = *fcc* + Fe_2B + TiB_2	E_1	1166	0.94	3.90
L = *fcc* + TiB_2 + *l*	E_2	1068	20.67	2.58

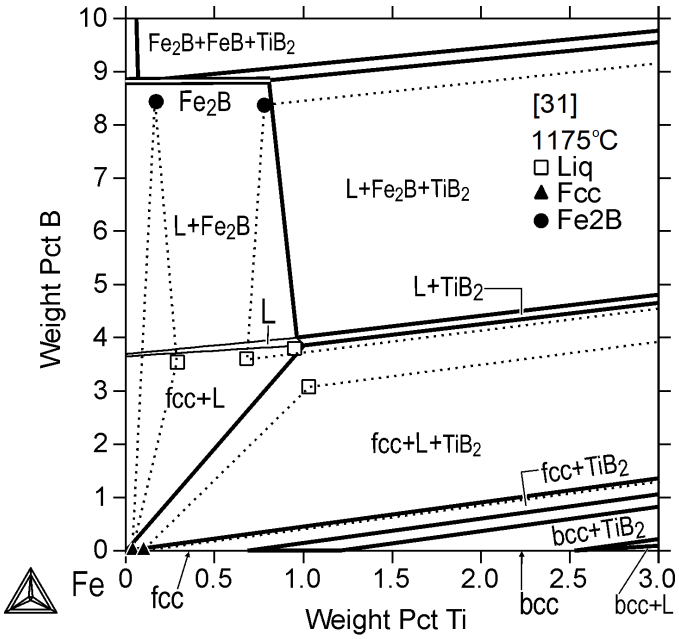

Fig. 10. Calculated isotherm of 1175°C in the Fe-B-Ti system, together with experimental data points [31]

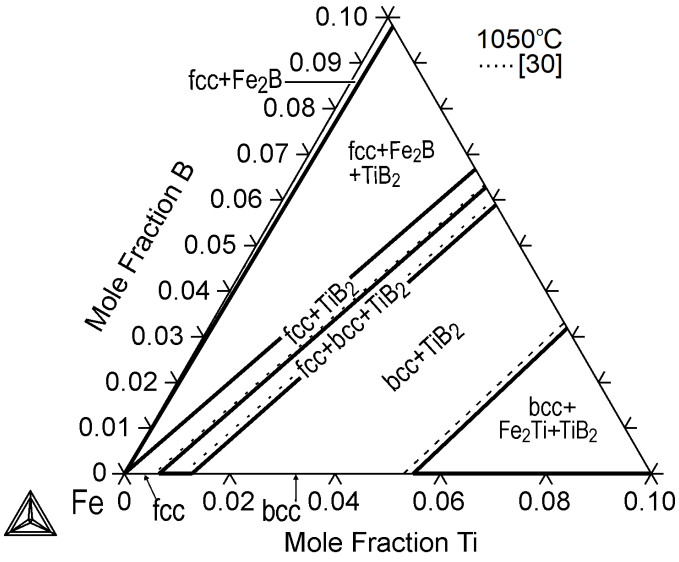

Fig. 11. Calculated isotherm of 1050°C in the Fe-B-Ti system, together with experimentally determined phase regions [30] (dotted lines)

4. Summary

A thermodynamic description was optimized for the ternary Fe-B-Ti system and its binary sub-system B-Ti, using the experimental thermodynamic and phase equilibrium data from the literature. The system Fe-Ti was reoptimized partially as well. In these descriptions, twelve phases, i.e., liquid, *bcc*, *fcc*, *hcp*, Fe_2Ti, FeTi, Fe_2B, FeB, TiB, Ti_3B_4, TiB_2 and beta-rhombo-B, were considered. The disordered solution phases, i.e., liquid, *fcc*, *bcc* and *hcp*, were described with the substitutional solution model, and all compounds, i.e, Fe_2Ti, FeTi, Fe_2B, FeB, TiB, Ti_3B_4, TiB_2, were treated as stoichiometric phases. In addition, no solubility of Fe and Ti was assumed in the beta-rhombo-B phase. A good correlation was obtained between the calculated and the experimental thermodynamic and phase equilibrium data.

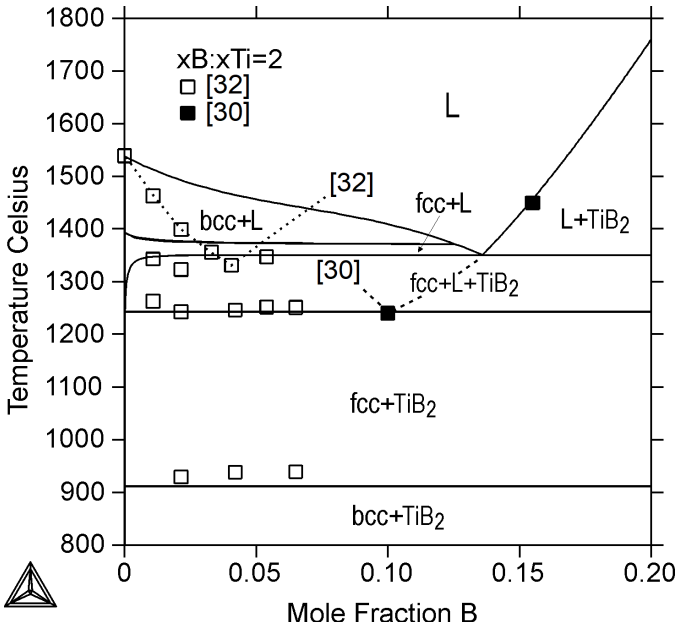

Fig. 12. Calculated vertical section in the Fe-B-Ti system at molar ratio x_B:x_{Ti} = 2, together with experimental data points [30,32]

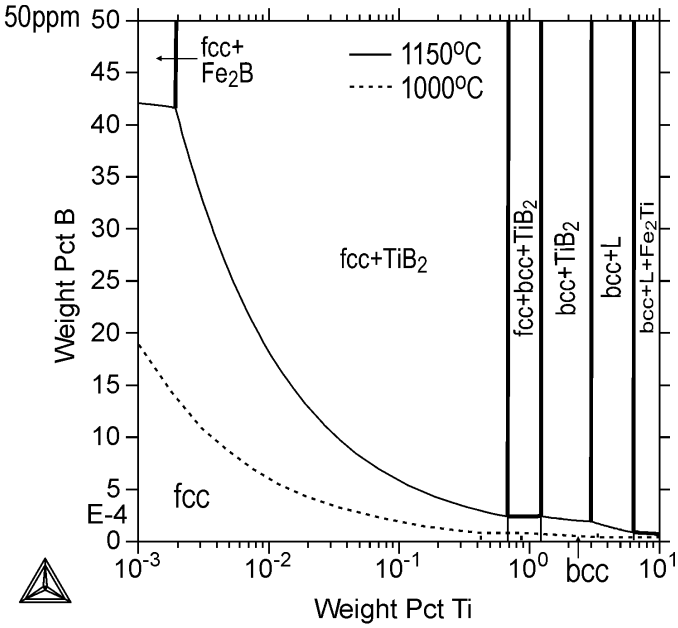

Fig. 13. Calculated B solubility in the *fcc* and *bcc* phases of the Fe-B-Ti system, at 1150 and 1000°C

Acknowledgement

This study was executed within the framework of the Genome of Steel profiling project. The Academy of Finland (project 311934) and Walter Ahlström Foundation are acknowledged for funding this work.

REFERENCES

[1] J. Miettinen, G. Vassilev, Arch. Metall. Mater. **59**, 601 (2014).
[2] J. Miettinen, G. Vassilev, Arch. Metall. Mater. **59**, 609 (2014).
[3] J. Miettinen, K. Lilova, G. Vassilev, Arch. Metall. Mater. **59**, 1481 (2014).
[4] J. Miettinen, V-V. Visuri, T. Fabritius, N. Milcheva, G. Vassilev, Arch. Metall. Mater. **64**, 451 (2019).
[5] J. Miettinen, S. Louhenkilpi, H. Kytönen, J. Laine, Math. Comput. Simulat. **80**, 1536 (2010).
[6] A. Burbelko, J. Falkus, W. Kapturkiewicz, K. Solek, P. Drozdz, M. Wrobel, Arch. Metall. Mater. **57**, 379 (2012).
[7] L.F.S. Dumitrescu, M. Hillert, N. Saunders, J. Phase Equilibria, **19**, 441 (1998).
[8] B-J. Lee, Metall. Trans. A, **32A**, 2423 (2001).
[9] H. Bo, J. Wang, L. Duarte, C. Leinenbach, L-B. Liu, H-S. Liu, Z-P. Jin, Trans. Nonferr. Met. Soc. China, **22**, 2204-11 (2012).
[10] K. Tanaka, T. Saito, J. Phase Equilibria, **20**, 207 (1999).
[11] C. Bätzner, In COST 507 – Thermochemical database for light metal alloys, Volume 2, I. Ansara, A.T. Dinsdale, M.H. Rand eds., European Communities, Belgium, 1998.
[12] X. Ma, C. Li, Z. Du, W. Zhang, J. Alloys and Compounds **370**, 149 (2004).
[13] V.T. Witusiewicz, A.A. Bondar, U. Hecht, S. Rex, T.Ya. Velikanova, J. Alloys Compd. **448**, 184 (2008).
[14] C. Qiu, Thermodynamic study of carbon and nitrogen in stainless steels. Ph.D. Thesis, Royal Institute of Technology, Stockholm, 1993.
[15] C. Qiu, Z-P. Jin, Scripta Metall. **28**, 85 (1993).
[16] V. Raghavan, Phase Diagrams of Ternary Iron Alloys – Part 6A, Indian Institute of Metals, Calcutta, **430** (1992).
[17] V. Raghavan, J. Phase Equilibria, **24**, 455 (2003).
[18] E. Rudy, USAF Tech. Report AFML-TR-65-2. Part V, Wright Patterson AFB, OH 1969.
[19] J.L. Murray, P.K. Liao, K.E. Spear, Bulletin of Alloy Phase Diagrams **7**, 550 (1986).
[20] L. Brewer, H. Haraldsen, J. Electrochem. Soc. **102**, 399 (1955).
[21] P.O. Schissel, W.S. Williams, Bull. Am. Phys. Soc. Ser. II, **4**, 519 (1959).
[22] P.O. Schissel, O.C. Trulson, J. Phys. Chem. **66**, 1492 (1962).
[23] V.V. Akhachinskij, N.A. Chirin, Thermodynamic of Nuclear Materials 1974, Vol. 2, IAEC, Vienna, 1975.
[24] T.J. Yurick, K.E Spear, Thermodynamic of Nuclear Materials 1974, Vol 1, IAEA-SM-236/53, 1980.
[25] L. Guzman, M. Elena, A. Miotello, P.M. Ossi, Vacuum **46**, 951 (1995).
[26] E.T. Turkdogan, Physical chemistry of high temperature technology, Academic Press, New York, 1980.
[27] Smithells Metals reference book, 8th edition, W.F. Gale and T.C. Totenmeier eds., Elsevier Butterwords Heinemann, New York, 2004.
[28] M.W. Chase, NIST-JANAF Thermochemical Tables, 4th.ed. American Institute of Physics for the National Institute of Standards and Technology, 1998.
[29] D.R. Stull, H. Prophet, JANAF Thermochemical Tables, 2nd ed., Nat. Stand. Ref. Data Ser., Nat. Bur. Stand, US, 1971.
[30] L. Ottavi, C. Saint-Jours, N. Valignant, C-H. Allibert, Z. Metallkd., **83**, 80 (1992).
[31] A. Antoni-Zdziobek, M. Gospodinova, F. Bonnet, F. Hodaj, J. Alloys and Compounds, **657**, 302 (2016).
[32] A.K. Shurin, V.E. Panarin, Russ. Metall. **5**, 192 (1974).
[33] A.D. McQuillan, J. Inst. Met. **79**, 71 (1951).
[34] H.W. Worner, J. Inst. Met. **79**, 173 (1951).
[35] R.J. van Thyne, H.D. Kessler, M. Hansen, Trans. ASM**44**, 974 (1952).
[36] A. Hellawell, W. Hume-Rothery, Philos. Trans. R. Soc. London, **249**, 417 (1957).
[37] S.H. Moll, R.E. Ogilvie, Trans. AlME **215**, 613 (1959).
[38] Y. Murakami, H. Kimura, Y. Nishimura, Trans. Nat. Res. Inst. Met. **1**, 7 (1959).
[39] T. Wada, Trans. Nat. Res. Inst. Met.**6**, 43 (1964).
[40] E.P. Abrahamsson, S.L. Lopeta, Trans. Met. Soc. AIME **236**, 76 (1966).
[41] W.A. Fisher, K. Lorentz, H. Fabritius, A. Hoffman, G. Kalwa, Arch. Eisenhüttenwes. **37**, 79 (1966).
[42] A. Balesius, U. Gonser, J. Phys. Colloq. **37**, C6/397 (1976).
[43] M. Ko, T. Nishizawa, J. Jpn Inst. Met. **43**, 118 (1979).
[44] J. Matyka, F. Faudot, J. Bigot, Scripta Metall. **13**, 645 (1979).
[45] M.M. Stupel, M. Bamberger, M. Ron, J. Less-Common Met. **123**, 1 (1986).
[46] J.K. Kivilahti, O.B. Tarasova, Metall. Trans. A, **18A**, 1679 (1987).
[47] G.I. Batalin, V.P. Kurach, V.S. Sudavtsova, Russ. J. Phys. Chem. **58**, 289 (1984).
[48] H. Wang, R Luck, B. Predel, Z. Metallkd. **82**, 659 (1991).
[49] U. Thiedemann, J.P. Qin, K. Schaefers, M. Rösner-Kuhn, M.G. Frohberg, ISIJ Int. **35**, 18 (1995).
[50] R.J. Fruehan, Metall. Trans. **1**, 3403 (1970).
[51] T. Furukawa, E. Kato, Trans. ISIJ, **16**, 382 (1976).
[52] J.C. Gachon, M. Notin, J. Hertz, Thermochim. Acta **8**, 155 (1981).
[53] A.T. Dinsdale, T.G. Chart, F.H. Putland, NPL Report DM(A) 96 (1985).
[54] A.T. Dinsdale, SGTE unary database, version 4.4; www.sgte.net A.T. Dinsdale, CALPHAD **15**, 317 (1991).
[55] B. Hallemans, Wollants, J.R. Roos, Z. Metallkd. **85**, 676 (1994).
[56] I. Ansara, A.T. Dinsdale, M.H. Rand, COST 507 – Thermochemical database for light metal alloys, Volume 2, European Communities, Belgium 1998.
[57] J-O. Andersson, T. Helander, L. Höglund, P. Shi, B. Sundman, CALPHAD **26**, 273 (2002).
[58] L.G. Voroshin, L.S. Lyakhovich, G.G. Panich, G.F. Protasevich, Met. Sci. Heat Treat. (USSR) **9**,732 (1970).